Conceptual Design of Cable Driven Parallel Mechanism for Planar Earthquake Simulator

Daisuke Matsuura[1], Shota Ishida[1], Muhamad Akramin[1], Emek Barış Küçüktabak[1], Yusuke Sugahara[1], Yukio Takeda[1], Nobuo Fukuwa[2] and Minoru Yoshida[3]

[1] Department of Mechanical Sciences and Engineering, Tokyo Institute of Technology, Tokyo, Japan
[2] Disaster Mitigation Research Center, Nagoya University, Nagoya, Japan
[3] Hakusan Corporation, Tokyo, Japan

1. Introduction

Numbers of massive earthquakes occurred globally in the past decades. One of the significant example is the Great East Japan Earthquake in 2011 with a magnitude of 9.0. The occurrence of earthquake cannot be prevented, but its effect towards public can be reduced by several means. Earthquake simulator is helpful for society to experience real seismic waves in safe environment. This can be used to raise awareness toward disaster (prevention). Cable-driven parallel mechanisms offer remedy to some shortcomings of conventional serial and parallel mechanisms (Gosselin, 2014). Using cables, it offers large workspace, low inertia of moving parts, transportability and ease of assembly/disassembly. These advantages of cable-driven parallel mechanisms are practical for an earthquake simulator that is accessible to public.

Earthquake Simulator Vehicle, Kishinsha (Masaki, 2013) is one of the simulators that is widely used for the purpose of disaster prevention education in Japan. It is good in term of transportability but can reproduce limited types of seismic wave. E-Defence (Ohtani, 2004) can reproduce various types of seismic wave with high precision. This simulator has a 20 m×15 m moving platform which is driven by forteen hydraulic actuators. Due to its massive size, this simulator is lack of transportability. Jishin-The-Vuton (Roh et al, 2013) is very excellent in term of transportability. Its driving principle is based on the VUTON crawler, developed by Hirose (Hirose, 1993), to reproduce seismic waves in two-dimensional plane. By using the crawler, the simulator can achieve wide range of motion. As a drawback, this simulator is prone to tipping due to difference in height of the center of gravity of the moving parts and the driving mechanism (crawler).

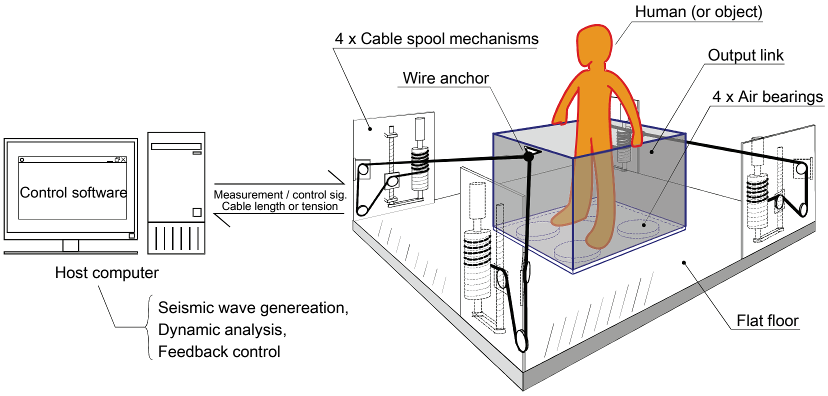

Figure 1. Conceptual drawing of planar earthquake simulator.

In order to develop an earthquake simulator with high transportability performing wide range of seismic waves in plane, a composition of simulator has been proposed (Shiwaku et al, 2012). The proposed design was composed of a parallel mechanism driven by four cables arranged in a plane and air bearings to reduce the friction. After this, we have succeeded this project to develop a simulator of real size. There are numerous examples of research regarding cable driven parallel mechanisms (Khakpour et al, 2014) (Liu et al, 2014) (Babaghasabha et al, 2015), however, to the best knowledge of the authors, researches aiming at development of earthquake simulator involving massive load and high acceleration have not been successfully done yet.

Following the introduction, the conceptual design of planar earthquake simulator is presented, which is composed of a cable driven parallel mechanism with four cables, flat floor and air bearings to support the mechanism with low friction. Cable arrangement is investigated by dynamic simulation with respect to stability. Finally, a prototype design is presented.

2. Composition of Planar Earthquake Simulator

Figure 1 shows the concept of our planar earthquake simulator. It is composed of a cable driven parallel mechanism (CDPM) with four cables, a flat floor and four air bearings. Object or human occupant are put on the output link of CDPM to experience simulated earthquake. As the first step, our target is to achieve big earthquake motions in the horizontal plane. To this end, the four air bearings are arranged between the output link of CPDM at each corner and the flat floor. This composition

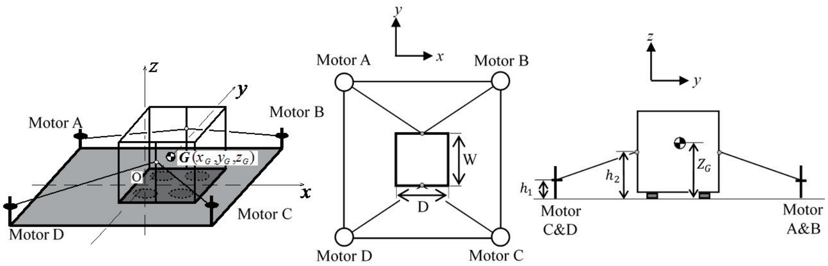

(a) isometric view (b) top view (c) side view

Figure 2. Arrangement of cables of CDPM.

contributes to a stable support of the output link to prevent tipping by small cable tension forces and smooth and fast motion with low friction.

The arrangement of the cables is shown in Fig. 2. To achieve full motion control of the output link in the horizontal plane, four cables are used. As shown in the side view (Fig. 2(c)), the heights of the attachment points of cables on the base, h_1, and the output link, h_2, are not the same, which is the main difference of the present mechanism configuration from that of the previous one. This means, our proposed CDPM has a spatial cable arrangement and a constraint plane (planar pair is composed of air bearings and flat floor) to achieve stable, smooth and fast motions in a plane. The effect of this configuration is investigated through dynamic simulations in the following section.

3. Dynamic Simulations

Dynamic model of the CDPM is shown in Fig. 3. $\boldsymbol{F_A}, \boldsymbol{F_B}, \boldsymbol{F_C}$ and $\boldsymbol{F_D}$ are the cable tension forces applied on points S_1 ($\boldsymbol{F_A}$ and $\boldsymbol{F_B}$) and S_2($\boldsymbol{F_C}$ and $\boldsymbol{F_D}$) , $\boldsymbol{f_{b1}}$, $\boldsymbol{f_{b2}}$, $\boldsymbol{f_{b3}}$ and $\boldsymbol{f_{b4}}$ are the bearing forces, applied on points B_1, B_2, B_3 and B_4, respectively. $\boldsymbol{N_1}, \boldsymbol{N_2}, \boldsymbol{N_3}$ and $\boldsymbol{N_4}$ are the reaction forces between ground and air bearings, $\boldsymbol{f_k}$ is the kinetic friction force and μ_k is the kinetic friction coefficient. To simplify the equations, instead of four different reaction forces, their equivalent, $\boldsymbol{N_{eq}}$ is used. $\boldsymbol{N_{eq}}$ is applied on point N, and its x and y positions with respect to the center of mass of the output link G are denoted as x_N and y_N. Greater net moment from other forces with respect to x and y axes, causes the position of N to be further; thus, makes it more prone to tipping.

For a planar motion, dynamic equations become as follows:

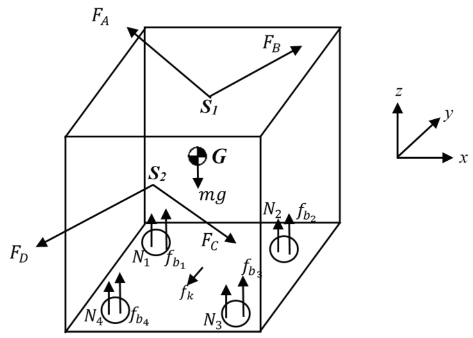

Figure 3. Dynamic model of CDPM with air bearings.

$$m\begin{bmatrix}\ddot{x}_G\\ \ddot{y}_G\\ 0\end{bmatrix} = \boldsymbol{F_A} + \boldsymbol{F_B} + \boldsymbol{F_C} + \boldsymbol{F_D} + \boldsymbol{f_{b_1}} + \boldsymbol{f_{b_2}} + \boldsymbol{f_{b_3}} + \boldsymbol{f_{b_4}} + \boldsymbol{N_{eq}} + \boldsymbol{f_k} + mg\begin{bmatrix}0\\ 0\\ -1\end{bmatrix} \tag{1}$$

$$\boldsymbol{I}\begin{bmatrix}0\\ 0\\ \ddot{\psi}\end{bmatrix} = (\boldsymbol{GS_1} \times \boldsymbol{F_A}) + (\boldsymbol{GS_1} \times \boldsymbol{F_B}) + (\boldsymbol{GS_2} \times \boldsymbol{F_C}) + (\boldsymbol{GS_2} \times \boldsymbol{F_D}) + (\boldsymbol{GB_1} \times \boldsymbol{f_{b_1}}) + (\boldsymbol{GB_2} \times \boldsymbol{f_{b_2}}) + (\boldsymbol{GB_3} \times \boldsymbol{f_{b_3}}) + (\boldsymbol{GB_4} \times \boldsymbol{f_{b_4}}) + (\boldsymbol{GN} \times \boldsymbol{N_{eq}}) + (\boldsymbol{GN} \times \boldsymbol{f_k}) \tag{2}$$

$$|\boldsymbol{f_k}| = -|\boldsymbol{N_{eq}}|\mu_k \tag{3}$$

Since the system is redundantly actuated for a planar motion; to have a unique solution, one of the cable tensions, $F_C = |\boldsymbol{F_C}|$ is preliminary determined. Bearing forces, physical, kinematic and dynamic parameters are the known parameters. Unknown parameters are the magnitudes of three cable forces, $|\boldsymbol{N_{eq}}|$,$|\boldsymbol{f_k}|$, x_N and y_N. These seven unknowns can be solved by using the seven scalar equations from equations (1), (2) and (3).

Dynamic simulations have been carried out. Standard values of physical, kinematic and dynamic parameters used in the simulations are shown in Table 1. Simulation results in Figs. 4 and 5 show how cable tension forces, friction force, magnitude and position of the equivalent normal force change with respect to h_1 and kinetic friction coefficient, for two different z_G values. In Fig. 4, the ideal case when the heights of the center of gravity, z_G, and the cable attachment point, h_2, are equal is considered. From this result, it is known that position of $\boldsymbol{N_{eq}}$ is independent from the height difference of cable attachment points and gets further

Table 1. Parameter values for simulation.

Parameter	Value	Parameter	Value	Parameter	Value
m	40 kg	F_C	400 N	$\ddot{x}_G$	9.8 m/s^2
W	1 m	x_G	-0.8 m	$\ddot{y}_G$	0
D	1 m	y_G	0	ψ	0
h_2	0.7 m	$\dot{x}_G$	0.1 m/s	$\dot{\psi}$	0
f_b	95 N	$\dot{y}_G$	0	$\ddot{\psi}$	0

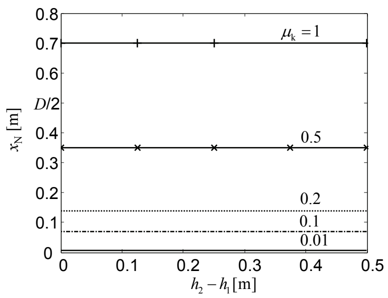

(a) x_N vs. $h_2 - h_1$

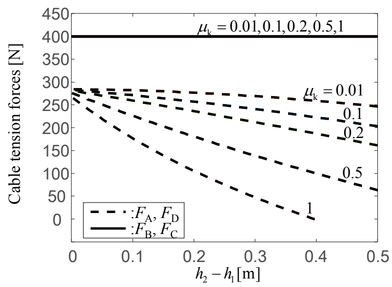

(b) Cable forces vs. $h_2 - h_1$

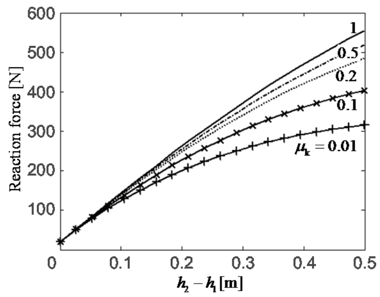

(c) N_{eq} vs. $h_2 - h_1$

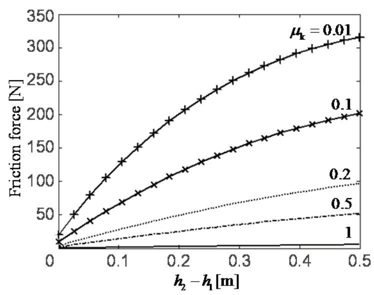

(d) Friction force vs. $h_2 - h_1$

Figure 4. Simulation results (home position, $z_G = h_2 = 0.7$ m).

from the center as the μ_k increases. In Fig. 5, the case when $z_G \neq h_2$ which should occur in practical usage is considered, where $z_G = 0.65$ m and $h_2 = 0.7$ m. In Fig. 5(a), hatched area shows the safe region without tipping. It can be seen that as the difference $h_2 - h_1$ decreases, output link gets more prone to tipping.

By comparing the results in Figs. 4 and 5, it is known that magnitudes of the cable tension forces, normal force and friction force are not dependent on the

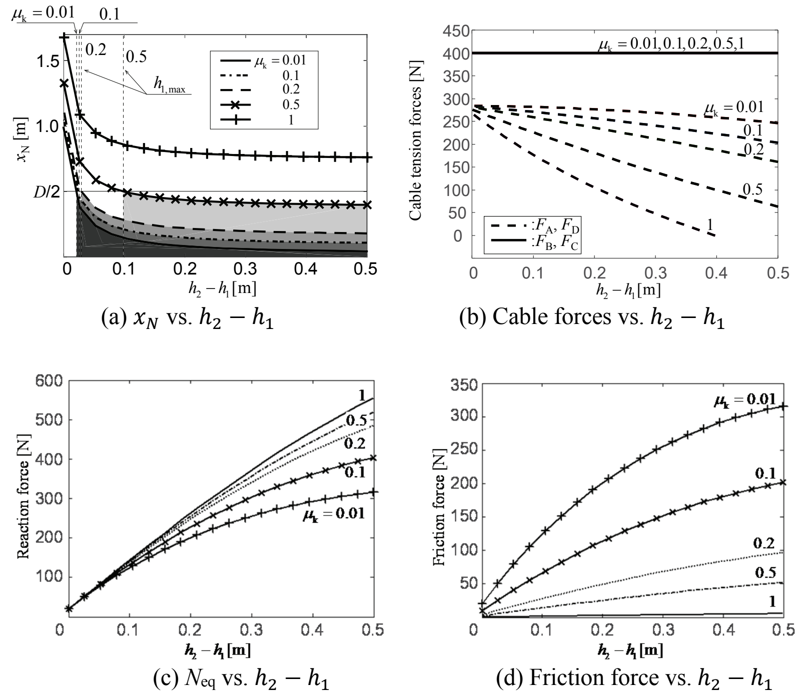

(a) x_N vs. $h_2 - h_1$ (b) Cable forces vs. $h_2 - h_1$

(c) N_{eq} vs. $h_2 - h_1$ (d) Friction force vs. $h_2 - h_1$

Figure 5. Simulation results (home position, $z_G = 0.65$ m, $h_2 = 0.7$ m).

height of the center of mass (z_G). In addition to this, it is also known that the height h_1 has a maximum limit, $h_{1,max}$, to prevent tipping. The effect of the difference $h_2 - z_G$ on $h_{1,max}$, is summarized in Fig. 6. Since there is no practical $h_{1,max}$ value for high coefficient of friction cases, which can also be seen in Fig. 4(a) and Fig.5(a), values of $\mu_k \leq 0.2$ are investigated. From this result, it is seen that if the friction coefficient is high, it's better to select h_2 smaller than z_G, whereas if μ_k is small, higher h_2 leads to more safe. It is worth noting that the effect of the coefficient of friction, in terms of tipping, decreases as the difference between h_2 and z_G decreases.

On the basis of these results, to have the most stable system, setting the physical parameters as follows is suggested. To decrease the possibility of tipping, h_1 should be set as low as the physical constraints allow. By using a lower coefficient of friction, cable tension forces can be kept in a desired region without loosening; however, it is important to make the connection point higher than the center of mass to obtain the most stable system in practice when the coefficient of friction is low.

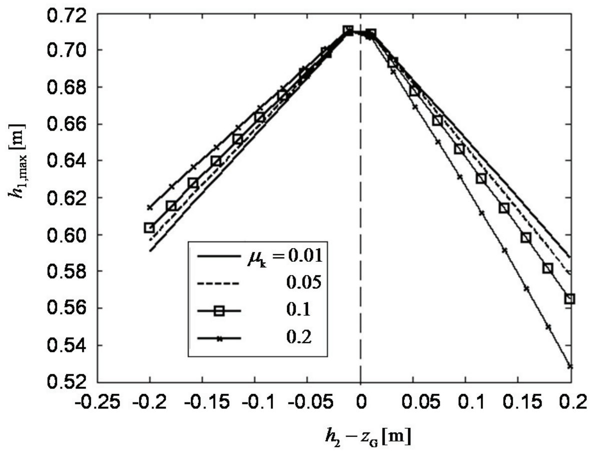

Figure 6. Relationship between $h_2 - z_G$ and $h_{1,max}$.

4. Prototype simulator

Based on the results mentioned above, we build a prototype. As one of the key parts of CDPM, the composition of a cable spool mechanism with the overview of our prototype earthquake simulator is shown in Fig. 7. The width and depth of the prototype are approximately 3.2 m each, and the height is 1.5 m approx. The cable spool mechanism is driven by a 400W brushless DC servomotor with a planetary gear head of reduction ratio 1/14 (EC60/GP81, Maxon motor ag). The actuator units are driven by servo amplifiers (1BLDC, HiBot corp.) to adjust the lengths of the four cables calculated by using pulse encoder signals of 500PPR with a PID feedback process. In addition, tension of the one of four cables is measured by a tension sensor (pickup: LSP10-K25-B-S and amplifier: T300, Eiko Sokki corp.) to maintain it to a specific value. All the above sensor signal processing, dynamic analysis and feedback control is performed by a PC-based controller (Intel Core- .5GHz, 16GB RAM, operated by Windows-7 Enterprise Edition) at 1kHz frequency triggered by a hardware timer interruption.

5. Conclusions

Conceptual design of an earthquake simulator using cable driven parallel mechanism is presented. To achieve seismic motions with high stability, spatial arrangement of

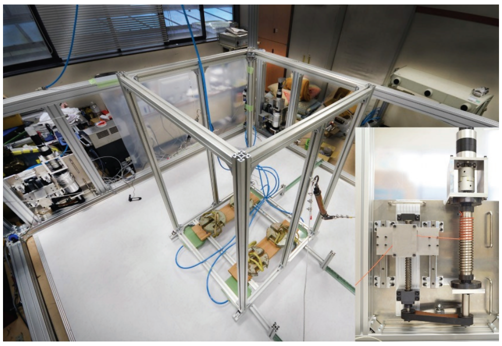

Figure 7. Overview of our prototype earthquake simulator and cable spool mechanism.

cables has been investigated. Prototype simulator which covers 1m stroke in each direction has been built.

Bibliography

Babaghasabha, R., Khosravi, M., A., Taghirad, H., D. (2015). Adaptive robust control of fully-constrained cable driven parallel robots. *Mechatronics*, vol. 25, 27-36.

Gosselin, C., M. (2014). Cable-driven parallel mechanisms: state of the art and perspectives. *Mechanical Engineering Reviews*, vol. 1, no. 1, doi: 10.1299/mer.2014dsm0004.

Hirose, S. and Amano, S. (1993). The VUTON: High payload, high efficiency holonomic omni-directional vehicle. In *Proceedings of the Sixth Symposium on Robotics Research*, 253-260.

Khakpour, H., Birglen, L and Tahan, S.A. (2014), Synthesis of Differentially Driven Planar Cable Parallel Manipulators. *IEEE Transaction on Robotics*, vol. 30, n.3, 619-630.

Liu, H., Gosselin, C., M. and Laliberte, T. (2014), Conceptual Design and Static Analysis of Novel Planar Spring-Loaded Cable-Loop-Driven Parallel Mechanisms. *Journal of Mechanism and Robotics*, vol. 4., n. 2, doi: 10.11151/1.4005568

Masaki, Y. (2013). Duration of "feeling of being shaken" as Assessed Using an Earthquake Simulator Vehicle. *Equilibrium Research*, vol. 72, 459-466.

Ohtani, K., Ogawa, N., Takayama, T. and Shibata H. (2004). Construction of E-Defense (3-D full-scale earthquake testing facility). *Thirteenth World Conference on Earthquake Engineering*, 189.

Roh, S.G., Taguchi, Y. Nishida, Y., Yamaguchi, R., Fukuda, Y., Kuroda, S., Yoshida, M. , Fukushima, E. F. and Hirose, S. (2013). Development of the portable ground motion simulator of an earthquake. *IEEE International Conference on Intelligent Robots and Systems*, 5339-5344.

Shiwaku, K., Roh, S.G., Nishida, Y., Yoshida, M. and Hirose, S. (2012). Proposition of cable driven earthquake simulator with pneumatic levitation. *Proc. Robotic Society of Japan*, 98 (in Japanese).